

The Development of Vision in the Zebrafish (*Danio rerio*)

Stephen S. Easter, Jr., and Gregory N. Nicola¹

Department of Biology, University of Michigan, 830 N. University Avenue,
Ann Arbor, Michigan 48109-1048

We studied the development and maturation of the visual system by determining when zebrafish begin to see and to move their eyes. This information was correlated with the time courses of the development of the retina, the retinofugal projection, the retinal image, and the extraocular muscles, to obtain an integrated picture of early visual development. Two visual behaviors were monitored over 48–96 hr postfertilization (hpf). The startle response (body twitch) was evoked by an abrupt decrease in light intensity. The optokinetic response (tracking eye movements) was evoked by rotation of a striped drum. Visually evoked startle developed over 68–79 hpf, more than 20 hr after the onset of a touch-evoked startle. It was not seen in eyeless fish, excluding a role for nonretinal light senses. Tracking eye movements developed over 73–80 hpf. They were always in the direction of drum rotation, even when the fish had been light deprived from blastula stage, ruling out a “trial and error” period of learning to track the drum. The image formed by the ocular lens was examined in intact fish made transparent by suppressing the formation of melanin. The eye was initially far sighted and gradually improved, so that by 72 hpf the image plane coincided with the photoreceptor layer. The extraocular muscles assumed their adult configuration between 66 and 72 hpf. Thus, the retinal image and functional extraocular muscles appeared nearly simultaneously with the onset of tracking eye movements and probably represent the last events in the construction of this behavior. © 1996 Academic Press, Inc.

INTRODUCTION

The zebrafish embryo is now one of the standard animals in the study of vertebrate development, joining the chick, *Xenopus*, and the mouse. Early events, particularly gastrulation and morphogenesis, have been studied in detail, exploiting the powerful tools of *in situ* hybridization (to reveal the regional expression of early patterning genes) and lineage markers *in vivo* (to reveal cell movements). However, once the genes have regionalized the embryo and the cells have moved into their proper sites, much remains to be done in the construction of the free-living fish, and these later events have been less studied. An especially important step is the development of vision, which is essential both in capturing prey and in avoiding predation by others. Clark (1981) described the development of visual behavior beginning at 4 days postfertilization (dpf), when zebrafish begin to

catch moving prey. The present study examines the period before that and links visual behavior to its underlying mechanisms: retinal image formation, the formation of neural connections in the retina and brain, and the maturation of those muscles involved in certain visuomotor behaviors.

The ontogeny of the visual system has been well described at the cellular level. The first postmitotic retinal cells appear at about 28 hr postfertilization (hpf) (Nawrocki, 1985) and the first optic axons at about 30 hpf. These axons reach the presumptive optic tectum at about 48 hpf (Stuermer, 1988; Burrill and Easter, 1994), which is also the birthdate of the first cones (Nawrocki, 1985) and the time at which the mosaic of cone photoreceptors is first apparent (Larison and BreMiller, 1990). Opsin is first expressed about 50 hpf (Raymond *et al.*, 1995), and the first outer segments are seen around 60 hpf, on cones (Branchek and BreMiller, 1984). The growth of optic axons continues apace (Bodick and Levinthal, 1980; Wilson *et al.*, 1990) and by 72 hpf their arbors have covered the tectum and arborized at nine other sites (Burrill and Easter, 1994). The present study links these observations to behavioral and optical aspects of visual function.

¹ Present address: Department of Neuroscience, Case Western Reserve University School of Medicine, 2119 Abington Rd., Cleveland, OH 44106.

The two behaviors that we have monitored reveal different aspects of vision. Visual startle probably presages an escape response (Kimmel *et al.*, 1974) that would normally be evoked by a looming predator. The presence of visual startle demonstrates that the fish can distinguish light and dark across time, but says nothing about form vision, the distinction of light and dark across space. Tracking eye movements, hereafter called the optokinetic response (OKR), indicates form-vision, because the fish must be able to resolve the dark and light stripes if they are to be tracked. OKR implies that a retinal image of the stripes is present, that the photoreceptive cells and the cascade of synapses in and beyond the retina are functional, and that the muscles that move the eyes are innervated and able to contract. Although both startle and optokinetic responses depend on a functional retina and optic nerve, they are apparently mediated by different parts of the brain, because an ablation study in adult goldfish showed that the shadow-evoked startle depended on an intact optic tectum, while OKR did not (Springer *et al.*, 1977).

A retinal image of the outside world is essential if the fish is to derive visual information. We follow the development of this image, relate its quality to the mosaic of cones that sample it, and evaluate the possibility that the refractive state of the eye is dependent on visual experience, as has been shown to be the case in birds and mammals (reviewed by Wallman, 1993).

We provide the first multifaceted view of the onset of vision, an important sensory function that has been studied widely in the experimental embryological context for nearly 50 years. Our findings have significance both for the interpretation of the older literature and for results now being generated by genetic analysis of zebrafish development.

Some of these results have previously been reported in abstract form (Easter and Nicola, 1995).

METHODS

Fish

Zebrafish (embryos and larvae) were obtained from our own outbred colony (Wilson *et al.*, 1990). Briefly, adults were kept in aquaria at 26–29°C, in a controlled 14-hr light/10-hr dark cycle. They spawned soon after the onset of light, and the fertilized eggs were collected within 2 hr after light onset. Eggs with the same number of cells (range 2–8) were sorted into individual petri dishes containing embryo rearing solution (ERS: 0.004% CaCl₂, 0.0163% MgSO₄, 0.1% NaCl, 0.003% KCl, and a trace of methylene blue), and the dishes were labeled with the date and time of sorting and the number of cells and put in an incubator at 28.5°C. The cell number provides information about the exact time of fertilization, assuming that the first division occurred 0.75 hpf and the next three divisions occurred at 0.25-hr intervals thereafter (Westerfield, 1993). Over the range of ages that we used, a particular stage of development (e.g., as measured by the progress of optic axonal outgrowth) correlated well with age, with an uncertainty of about 2–3 hpf (Burrill and Easter, 1995).

The light/dark regimen varied. Most fish were reared in transparent petri dishes in an incubator with a transparent top, so they experienced a nearly natural light cycle of alternating light and dark phases. A few fish were reared in total darkness to assess the role of visual experience in the development of both optics and behavior. Embryos less than 24 hpf were placed inside petri dishes whose outsides had been spray painted black to block light entry, and the petri dishes were placed inside an incubator with an opaque cover. The dishes were uncovered immediately before the fish were to be examined.

Some fish were reared in ERS supplemented with 0.2 mM phenylthiocarbamide (1-phenyl-2-thiourea, Sigma), which retards the formation of melanin and therefore makes the fish transparent (Westerfield, 1993).

Behavioral Assays

Fish were viewed from above (Fig. 1) in a dissecting microscope and videotaped. Individual fish were removed, one at a time, from their home petri dish and placed alone in a petri dish containing the same medium as their home. All fish were used at only one age, for only one set of observations. Once under observation, they were exposed to various stimuli (see below) and returned to a separate container to ensure that they were not used twice. During the time in the viewing arena, which never exceeded 20 min, the temperature of their environment gradually cooled toward room temperature (typically about 20°C).

Startle. In this set of experiments, the embryos were always removed from their chorions and immersed in ERS. A startle response is defined here as any abrupt movement of the fish that occurred within 2 sec after stimulus onset. Two stimuli were used, mechanical and visual, and one sham stimulus. The mechanical stimulus was the tip of a dull dissecting needle manually applied lightly and briefly to the flank caudal to the eye. The visual stimulus was an abrupt interruption of a bright light (the tip of a fiber-optic illuminator above the fish), effected by closing a shutter between the light and the animal for about 1 sec. The luminance at the plane of the fish was measured with a photometer (UDT Model 370, with reflex viewing module and a photometric filter) and found to decrease from 14 Foot Lamberts when the shutter was open to 0.6 Foot Lamberts when it was closed. The sham visual stimulus was the shutter closure with the fiber-optic illuminator extinguished. All fish experienced all three, visual followed by mechanical followed by sham visual, according to the following schedule. Five visual stimuli were delivered at 30-sec intervals over 2 min. Following a 1-min interval, five mechanical stimuli were delivered at 30-sec intervals. After another 1-min interval, five sham visual stimuli were delivered at 30-sec intervals. A range of 5–20 animals were tested at each age: 48, 66–79 (at 1-hr intervals), and 96 hpf.

To control for the possibility that the light-evoked startle was mediated by a light sense not located in the lateral eyes (e.g., in the brain or the skin), eyeless fish were tested. Seven 75 hpf larvae were anesthetized in an aqueous solution of 0.2% tricaine methane-sulfonate (Sigma) and immobilized in a 1.2% agar solution, and their eyes were removed surgically. They were returned to their home petri dishes and tested 3 hr later (78 hpf) identically to the normals.

OKR. In this set of experiments, embryos were left inside their chorions, positioned for viewing from the dorsal side of the head. The optically clear egg shell did not interfere with the embryo's view, and it served the useful function of limiting the fish's move-

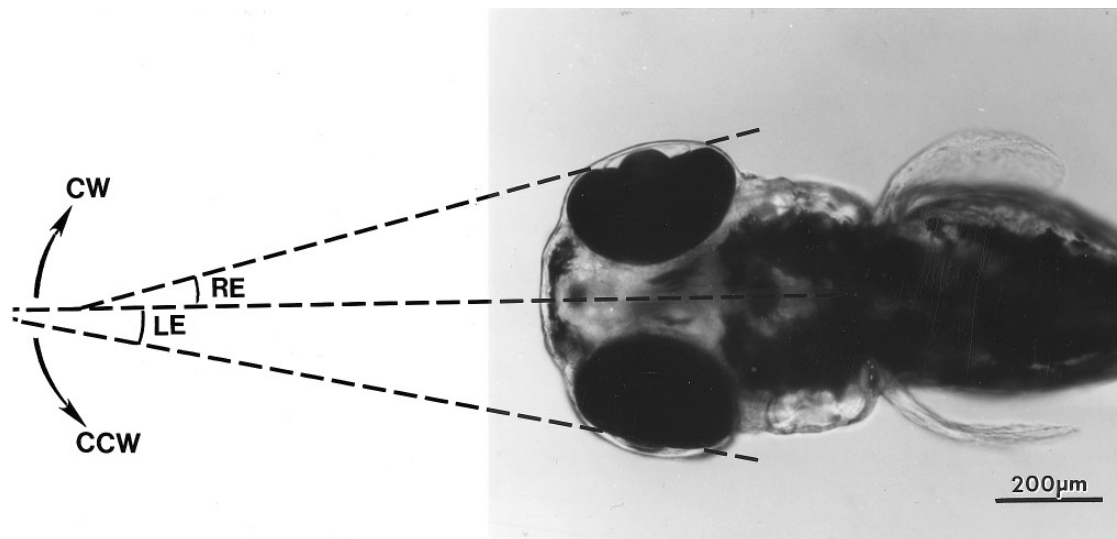


FIG. 1. Photomicrograph of a dorsal view of a fish viewed in the dissecting microscope. The lines indicate the body axis and the planes of the two pupils. The clockwise (CW) and counterclockwise (CCW) directions are indicated.

ment. The fish were placed in a specially constructed cylindrical glass chamber that rested on the center of the microscope stage. The chamber was 3.5 cm high, with an inner diameter of 1.0 cm. A microscope coverglass 2.0 cm above the base of the microscope stage divided the chamber horizontally in two, and both halves of the cylinder, above and below the platform, were filled with ERS to provide an optically homogeneous medium through which the fish viewed its surroundings. Concentric with the chamber was the striped drum (a cardboard cylinder, 4.8 cm in diameter and 7.5 cm high, linked by a belt drive to a variable-speed electrical motor). From the view of the fish, on the horizontal divider, the striped drum subtended 360° horizontally and 105° vertically, including parts of both superior and inferior visual fields. The inside of the drum was lined with alternating vertical black and white stripes, either 45° or 22.5° wide. The luminance of the white and black stripes were roughly 8 and 0.14 Foot Lamberts, respectively. The drum rotated around the vertical axis, either clockwise or counterclockwise, at velocities of 2.4 and $6.5^\circ/\text{sec}$.

Stimuli were presented in a standard sequence that included both velocities, directions, and stripe widths, as illustrated in Fig. 2. When a fish changed position, the stimulus presentation was interrupted, the fish was repositioned, and the stimulus presentation continued where it had been interrupted. Twenty fish were tested at each age: 48, 70–81 (1-hr intervals), and 96 hpf. The entire epoch was videotaped at 60 frames per second with simultaneous voice commentary to identify the particular animal and to note both the direction and the velocity of the drum. The videotapes were replayed later (with the audio portion of the record silenced, to prevent knowing if the drum was rotating), and horizontal eye movements were noted and in some cases measured (Fig. 1). Subsequently, these eye movements were related to the state of the drum at the time they occurred. With the playback speed at 60 frames per second (the same as recording), saccadic eye movements (the fast ones: Easter, 1971) were easily detected, but the tracking movements (the smooth ones: Easter, 1972) were often too slow to be

detected and could only be seen when playback was speeded up to 360 frames per second.

Retinal Image Formation

The image formed by the eye was investigated in phenylthiocarbamide-raised fish, viewed in differential interference contrast optics in the compound microscope. The absence of melanin allowed direct visual access to the back focal plane of the ocular lens. A specially constructed chamber was made by cutting a circular hole in thin plastic stock and gluing the plastic to a microscope slide to form a well about $250\ \mu\text{m}$ deep. The well was filled with ERS, and living fish, anesthetized or unanesthetized, were positioned therein, with one eye facing obliquely downward (see Fig. 7a), looking into the beam emerging from the substage condenser. A coverslip was firmly affixed to the top of the plastic ring with petroleum jelly, thus allowing good visual access to the well, which was deep enough that the fish were not squashed, but shallow enough to allow the microscope objectives ($10\times$ dry, $50\times$ water-immersion) to focus through the entire depth.

Anatomy

Ultrathin and semithin sections of fish of various ages were examined using general stains. Individuals were anesthetized in 0.1% tricaine methanesulfonate and prepared according to methods published earlier (Wilson *et al.*, 1990). Briefly, the fish were immersion-fixed in a phosphate-buffered mixture of paraformaldehyde and glutaraldehyde, postfixed in osmium tetroxide, bloc-stained with uranyl ions, and embedded in epon. They were sectioned at $1\ \mu\text{m}$ thickness and stained with toluidine blue for light microscopic examination. Ultrathin sections from the same blocks were cut, mounted on formvar-coated one-hole grids, stained with lead ions, and examined electron microscopically. Sections of the retina and

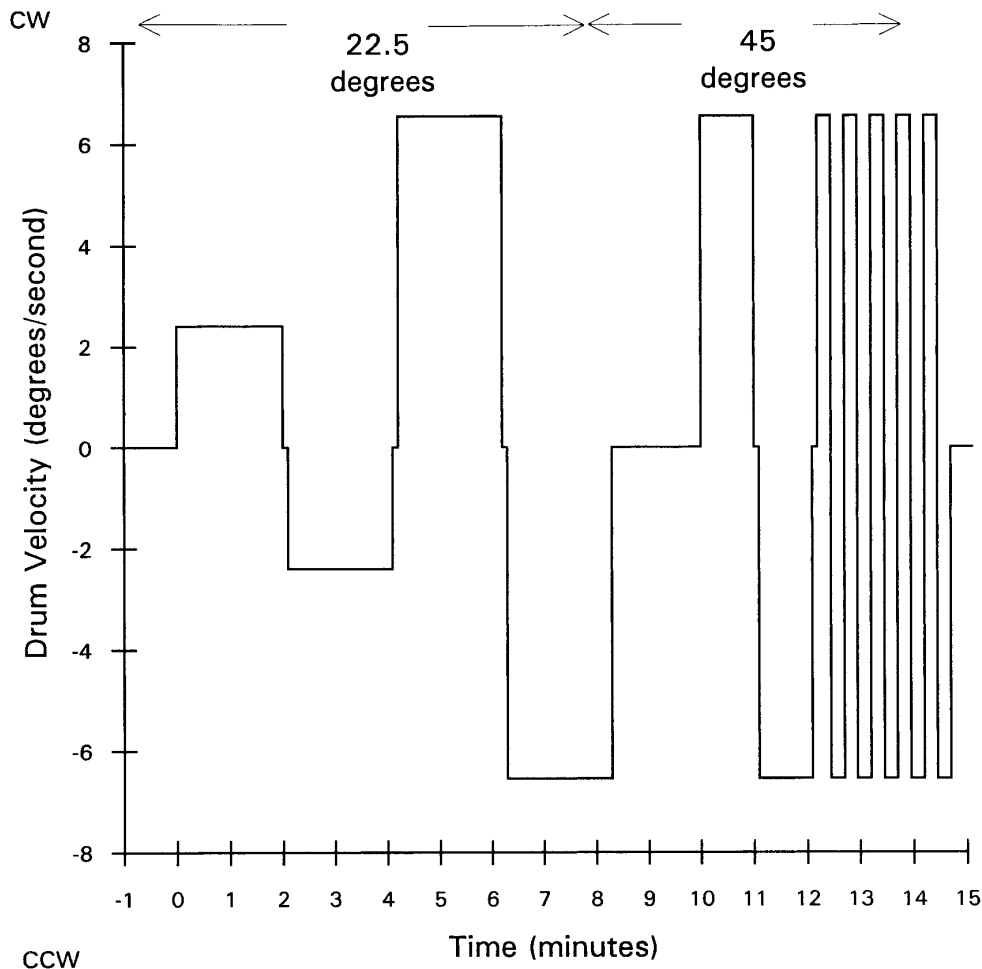


FIG. 2. Drum rotation sequence. The vertical axis shows the velocity of rotation and the horizontal axis the time. The arrows above indicate when the two sizes of stripes, 22.5 and 45° width, were in use. CW, clockwise; CCW, counterclockwise.

of the extraocular muscles were examined light- and electron-microscopically in normal 72 and 96 hpf fish. The pineal body was similarly examined in the eyeless 78 hpf fish that had been used in the control experiments for visual startle.

The monoclonal antibody ZM-1 (raised by Dr. W. Trevarrow; Westerfield, 1993) was used to label muscle tissue. Several individuals at each of the ages (48, 60, 66, 72, and 96 hpf) were anesthetized as above and labeled with the antibody according to methods published earlier (Wilson *et al.*, 1990). Briefly, they were immersion-fixed in phosphate-buffered paraformaldehyde and incubated either as whole mounts or frozen sections (20 μ m thick), followed by a peroxidase-conjugated secondary antibody and incubation in H_2O_2 plus diaminobenzidine. Sections were counterstained with toluidine blue and mounted under coverslips in DPX. Fish that were to be whole-mounted had been raised in phenylthiocarbamide which rendered them transparent. Whole mounts were cleared in xylene and mounted between two coverslips in DPX.

The anatomy of the living eye (especially the relations of the lens, retina, and cornea) was investigated in fish that had been

reared in phenylthiocarbamide. Intact treated fish, both anesthetized and unanesthetized, were immersed in ERS inside the same chambers that were described above. The eyes were examined in optical sections with the aid of differential interference contrast, which brings out individual cells and other landmarks such as the plexiform layers.

A stage micrometer was photographed for purposes of calibration in the light microscopy. The manufacturer's tables of magnifications were used to calibrate the electron micrographs.

RESULTS

Behavioral Studies

Startle Evoked by Touch and Shadow

The two startle responses had different times of onset, as Fig. 3 shows. The touch stimulus reliably produced a re-

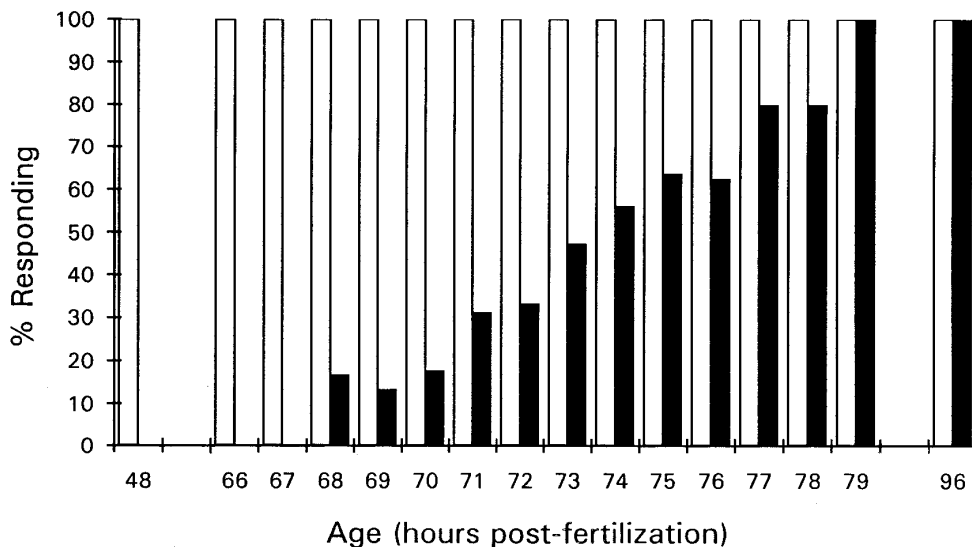


FIG. 3. Onset of touch- and shadow-induced startle. The vertical axis shows the percentage of animals (of 5–20 at each point) that responded to either touch (open bars) or interruption of light (solid bars). A positive response was scored if the subject responded to at least one of the five stimuli presented. The horizontal axis gives the ages of the subjects.

sponse in all fish of 48 hpf and older, confirming Grunwald *et al.* (1988), who described the response as early as 28 hpf. In contrast, no fish younger than 68 hpf ever responded to the shadow, and the percentage of responsive fish increased steadily from 17% at 68 hpf to 100% at 79 hpf.

Additional observations confirmed that the visual startle was caused by light on the retina. Electron microscopic examination of the retinas confirmed that photoreceptor outer segments were quite abundant by 72 hpf, and moreso by 96 hpf, confirming Branchek and BreMiller (1984), and that synapses were numerous in both the inner and outer plexiform layers (not shown); thus, the retinas were apparently functional. The sham light stimulus never evoked a response, so the shutter per se was not the effective stimulus. None of the eyeless fish responded to the light stimulus, in contrast to 80% of the intact fish of the same age (78 hpf). Electron microscopic examination of the eyeless fish revealed outer segments on the pineal photoreceptors (not shown), so the failure of the eyeless fish to respond to light cannot be attributed to incidental damage to this auxiliary photoreceptive structure. Because the eyeless fish responded normally to touch, the lack of visual startle in eyeless fish was not attributable to a general loss of irritability. We conclude that shadow must have evoked a response in the intact animals by way of the retina.

OKR

OKR developed gradually, beginning at 73 hpf. Fish younger than 72 hpf never made any spontaneous eye movements nor did they respond to the drum. Among the

73 hpf cohort, only 5% (1 of 20) responded, and this fraction increased steadily to reach 100% by 80 hpf (Fig. 4). Even among the responsive fish, tracking was quite episodic, as most of the time was spent not tracking the drum. Figure 5 shows a typical interlude during which a sluggish response in one eye was unaccompanied by a response in the other, but both eyes were unresponsive most of the time. Both the fraction of time spent tracking the drum and the velocity of the tracking movements increased up to 96 hpf, at which age the fish were responding continuously and tracking the drum with an accuracy that rivaled that of the adult (Easter and Nicola, unpublished). In summary, the onset of OKR was delayed about 5 hr after the visual startle response (73 hpf vs 68 hpf), but both responses reached 100% response at about the same age (80 hpf vs 79 hpf) and improved thereafter.

Observations of early OKR suggest that its neural substrate developed initially without the influence of visual experience. To explain, OKR is a reflex linking a stimulus (retinal image movement in a particular direction) to a response (eye movement in the same direction). The direction of image movement is converted into the appropriate direction of eye movement by a neural circuit, and the polarity must be correct, e.g., clockwise movement of the drum should evoke clockwise, and not counterclockwise, movement of the eyes. This polarity might be set independent of visual experience. Alternatively, it might be set on the basis of a functional validation of visual experience—when image movement is first sensed, move the eyes randomly and whatever direction of movement diminishes the movement of the retinal image will be adopted thereafter, roughly

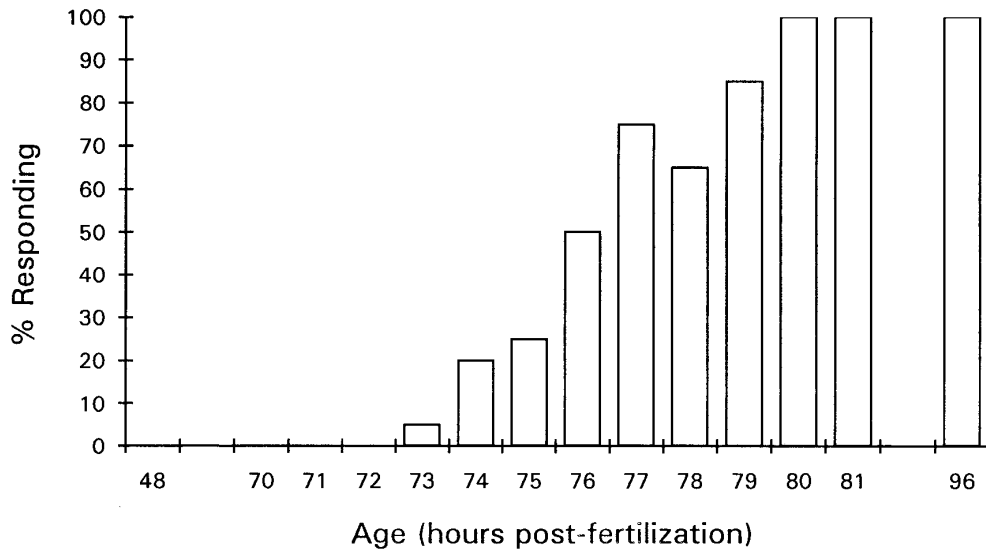


FIG. 4. Onset of OKR. The vertical axis shows the percentage of animals (of 20 at each point) that responded to the rotating drum with a tracking movement at some time during the trial period.

analogous to the higher order process of behavioral imprinting. If experience were essential, we would expect to see evidence of trial-and-error behavior, i.e., the drum rotation should evoke some eye movements in the wrong direction. Alternatively, if the polarity were set in advance, without reference to visual experience, we would predict no misdirected movements. We never saw any spontaneous slow movements in the absence of a rotating drum nor did we see any movements in the wrong direction when the drum was rotating. Although this result is consistent with

the lack of a role for visual experience, it is not unequivocally so, since the fish may have set its polarity on the basis of visual experience in the incubator prior to seeing the drum. This possibility was tested by depriving the fish of any visual experience prior to entering the drum environment; the dark-reared fish (5 dpf) made appropriately directed tracking movements within minutes of emerging from the dark, with no sign of misdirected movements. Thus, in the total absence of previous patterned visual stimuli, they responded appropriately, suggesting that the polar-

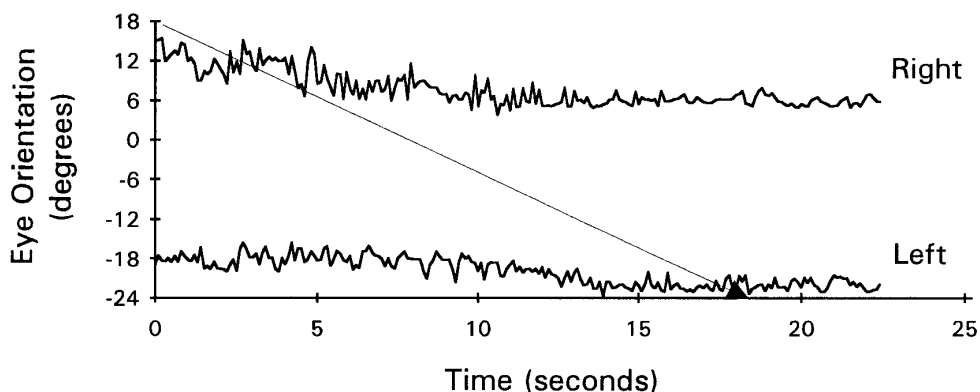


FIG. 5. OKR. The vertical axis shows the orientations of the eyes of a 76 hpf fish, sampled at 10 Hz, vs time on the horizontal axis. Throughout the 25-sec episode, the drum rotated clockwise at 2.5°/sec (see diagonal line) so if the eyes were tracking the drum accurately, they should have the same slope as the diagonal. During the initial 10 sec, the right eye rotated clockwise at about 1°/sec, and the left eye remained motionless. Over the remaining 15 sec, the right eye was motionless, and the left eye rotated clockwise initially and then stopped.

ity of OKR was hard-wired from the outset, independent of visual experience.

Retinal Image Formation

The delay of OKR relative to visual startle might be caused by the absence of a retinal image of the striped drum. We evaluated this possibility by investigating image formation in the developing eye, taking advantage of the optics of the compound microscope. With Köhler optics, the substage condenser's aperture diaphragm (SCAD), the aperture that is focused in the entry pupil of the microscope objective, is at optical infinity relative to the microscope stage. It follows that a positive lens at the stage will form a real inverted image of the SCAD at a distance equal to the focal length of the lens. A fish eye on the stage with its pupil facing the substage condenser should form an image of the SCAD, but the pigmented epithelium would normally absorb all the light entering the pupil and therefore block the objective's view of this image. In the absence of melanin, the rays of light that pass through the ocular lens are unimpeded down-beam, and whatever image they form can be directly visualized by the objective, no matter whether the image is inside or outside of the eye. If a fish eye is positioned on the stage, its pupil toward the light source, then the questions for our purposes are whether an image of the SCAD is formed by the eye, and, if so, at what plane is it formed?

In fish older than 72 hpf, a sharp image was evident at the plane of the photoreceptor/pigmented epithelium interface, which is the site of the receptor outer segments and therefore the appropriate location for the image. The pigmented epithelium is very thin at these ages and for that reason marks quite accurately the layer of photoreceptor outer segments. The pigmented epithelium also has certain textural features that, despite the absence of melanin, are enhanced by differential interference contrast microscopy, which made this interface easy to identify. We estimate that it can be accurately determined to within about 2 μm . The images at this plane are illustrated in the surgically isolated eye of Figs. 6a and 6b. The image had the shape of the SCAD, the size of the image varied according to the size of the SCAD, and when the eye was moved in the plane of the microscope stage, the image also moved, remaining in the eye. Changes in the diameter of the field diaphragm (the one focused at the plane of the stage) had no effect on the size of the image or on its brightness, provided the entire eye was illuminated. Therefore, the image was formed by the eye, and more specifically by the ocular lens, which is the only optically active element in a fish's eye (Pumphrey, 1961; Charman and Tucker, 1973). Similar observations were made in intact fish, but a grating (a transparency with alternating opaque and clear stripes) was inserted into the condenser beam at a point close to optical infinity, because the bars of a grating are easier to evaluate than the boundary of the aperture. Figure 6c shows the resultant image of a grating inside the image of the SCAD in the eye of an intact 85 hpf

fish. As in the isolated eyes, the image lay at the plane of the photoreceptor/pigmented epithelium interface. The depth of field of the image was estimated by focusing the microscope objective up and down and noting the range over which the image of the grating was still visible; it was about $\pm 60 \mu\text{m}$ on either side of the optimal plane of focus. We believe that the retinal image quality is considerably better than Fig. 6c suggests, because isolated lenses, fresh from the eye, produced images that could be seen without intervening extraocular tissue, and they were very sharp indeed (Figs. 6d and 6e).

The time course of the development of the retinal image was determined by locating the three planes at the center of the lens, the grating image, and the photoreceptor/pigmented epithelium interface. The positions of all three planes were noted from the dial readings on the microscope focusing knob. If the eye is emmetropic (in focus for objects at infinity), the grating image and the photoreceptor/pigmented epithelium interface would coincide (Figs. 6a–6c); if the eye is myopic (near-sighted), the image would be inside the eye in front of the photoreceptor/pigmented epithelium interface; and if the eye is hyperopic (far-sighted), the image would be outside the eye. The three planes are illustrated schematically in Fig. 7a, and Figs. 7b–7d illustrate the appearance of the three planes in one fish. We examined the images in intact fish of the following ages: 24, 39, 62, 68, 72, 85, 108, and 136 hpf. In all cases, the fish were alive, with circulation throughout the body, including the eye. Some of the older fish were anesthetized to reduce their movements, but this did not seem to influence the results. We saw no image at 24 hpf. At 39 hpf, the distance from lens center to image was roughly four times the distance from lens center to photoreceptor/pigmented epithelium interface; the eye was hyperopic. At 62 hpf, the ratio of the two distances had decreased to roughly three, and at 68 hpf, the ratio had decreased to about two (Fig. 7). By 72 hpf, the planes of the photoreceptors and the image were indistinguishable, and at the older ages, this same condition was maintained (Figs. 6a–6c).

We also examined dark-reared fish to determine if visual experience played a role in the development of emmetropia. These fish had been raised in total darkness until immediately before they were put in the chamber and the planes of the best image and the photoreceptor/pigmented epithelium interface were located. The cones were more easily discerned in these older eyes, as they were larger and their inner segments were more refractile than in the younger fish. The two planes were coincident, which rules out a role for experience in the establishment of the focal length. In summary, the eye progressed from hyperopic to emmetropic by about 72 hpf, which, under natural conditions, would be the morning of the first day posthatch. This corresponds closely to the time of the first appearance of OKR, in support of the hypothesis that the delay in the onset of OKR was attributable to the late appearance of an image at the plane of the photoreceptor outer segments.

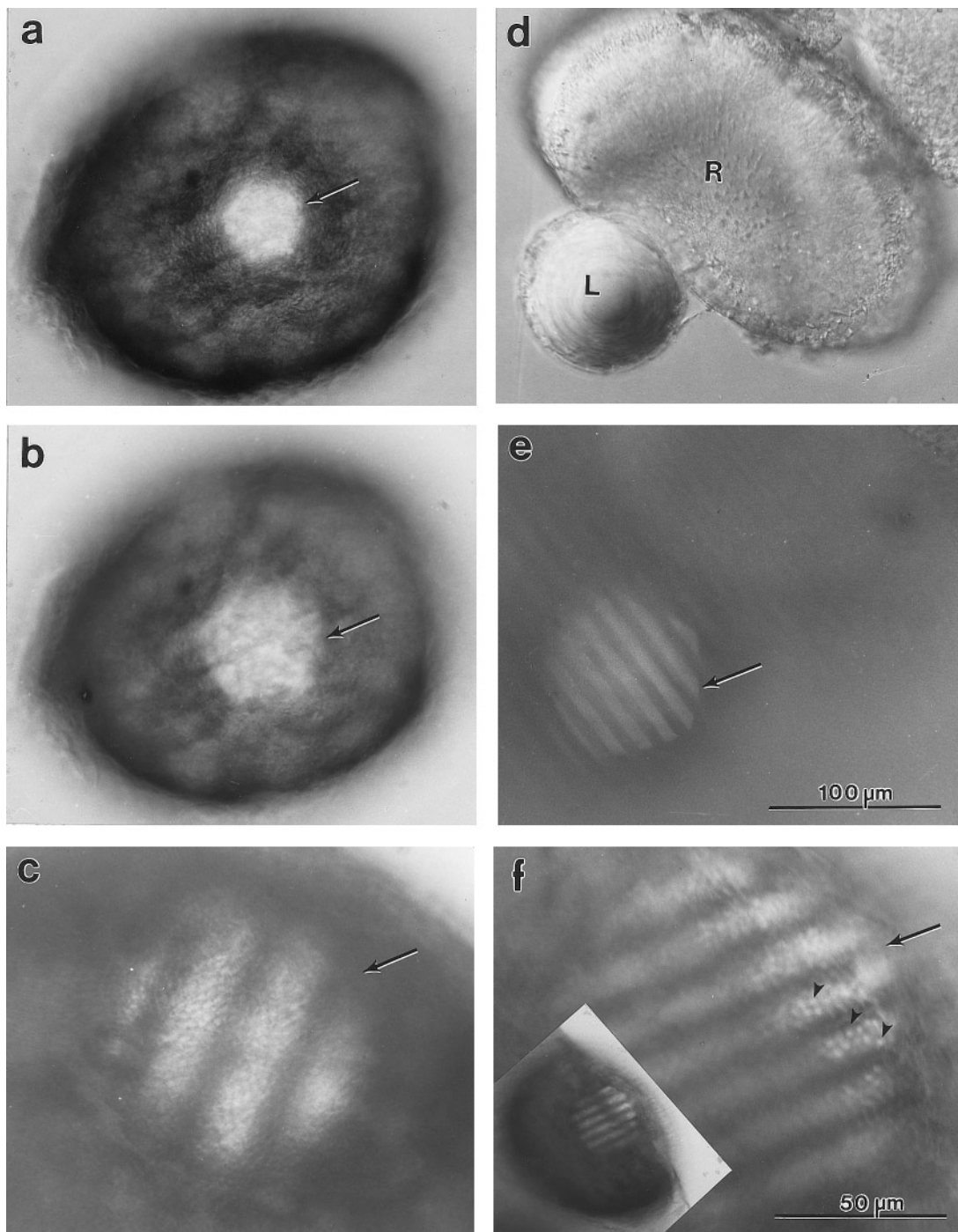


FIG. 6. Retinal image at the appropriate plane. Arrows indicate the edge of the image of the substage condenser aperture diaphragm (SCAD). (a–c) All three panels are micrographs of eyes, focused at the plane of the photoreceptor/pigmented epithelium interface. (a, b) These illustrate the same eye, from a 108 hpf fish, surgically isolated and positioned with the pupil looking into the condenser beam, away from the objective. The image of the SCAD is shown, pinched down in a and opened wide in b. (c) This is a dorsomedial view of a right eye in a live 85 hpf fish, lateral up and to the right, anterior up and to the left. The image of a grating inside the SCAD appears on the dorsal retina. The cone layer is evidenced in the granular texture, most visible in the bright stripes. (d, e) These are two views of the same field, at different planes of focus. (d) A freshly isolated lens (L) adheres to a fragment of the retina (R). The plane of focus is at the level of the lens center. (e) The plane of focus is at the back focal plane of the lens, showing a sharp image of a grating (finer than the one in c) inside a SCAD. (f) A dark-reared 128 hpf fish, showing that the image of the grating and the SCAD are in focus at the level of the cones, whose ellipsoids are visible (arrowheads). The inset shows a less magnified view of this same field. Scale bar in e applies to a, b, d, and e, and the one in f applies to c and f.

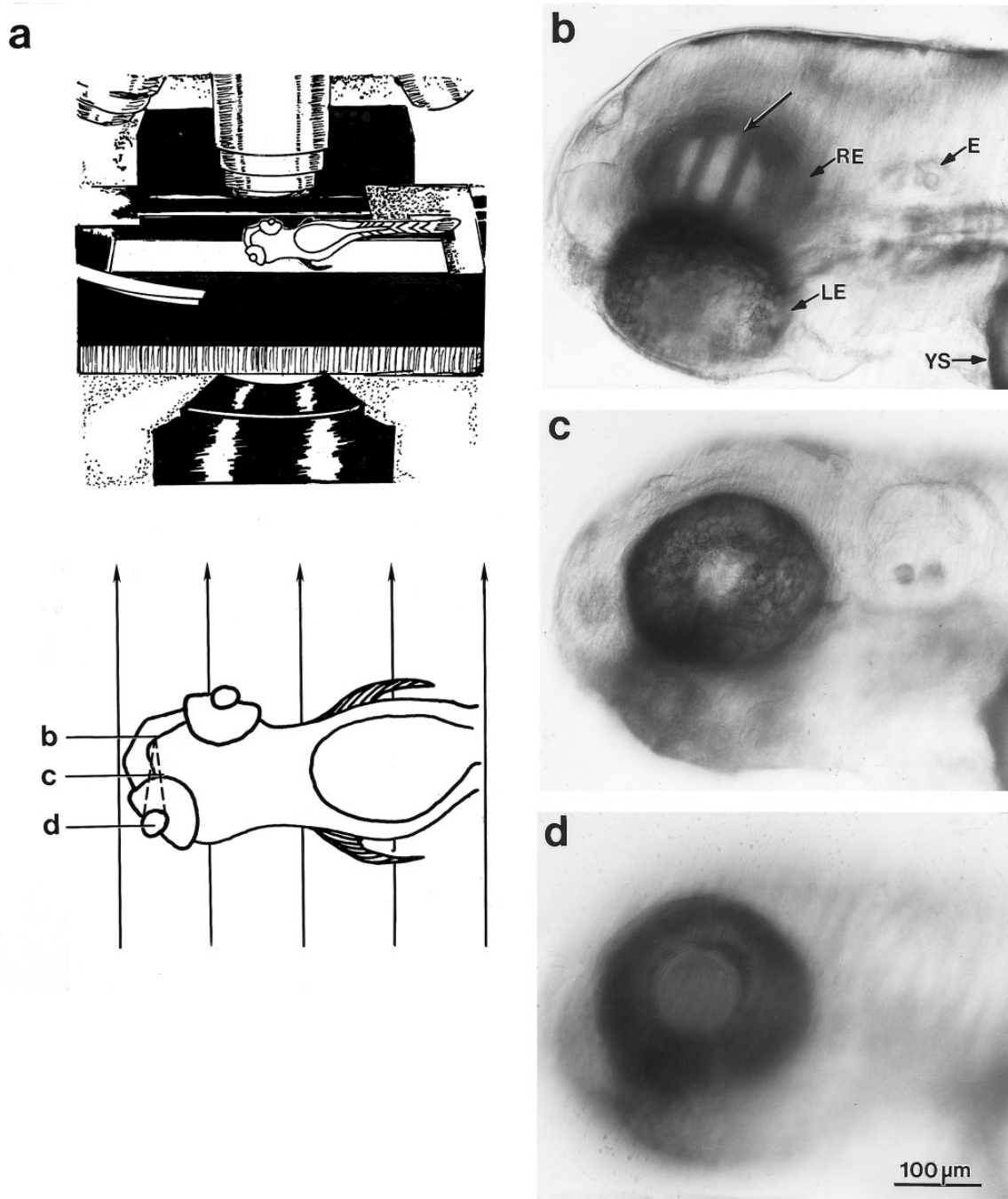


FIG. 7. Image at an inappropriate plane. (a) The upper sketch shows the setup; a larval zebrafish was positioned obliquely on a microscope slide, inside a water-filled chamber (not shown), with one eye oriented downward toward the condenser lens. The lower sketch shows the larva in more detail, with the parallel rays from the SCAD below indicated by the vertical arrows. The image of the SCAD is formed by the ocular lens at the location given by the convergence of the dashed lines. The letters b, c, and d indicate the planes at which the pictures in b, c, and d were focused (d, the lens center; c, the photoreceptor/pigmented epithelium interface; and b, the plane of the image of the grating). (b–d) These are photomicrographs of the same 68 hpf larva, anterior to the left, viewed dorsolaterally with the right eye (RE, toward the top) facing down and the left eye (LE) facing up. The yolk sac (YS) and ear (E) are indicated. The pictures were taken at the three different focal planes shown in a. The image (unlabeled arrow) lay behind the right retina, about twice as far from the lens center as the photoreceptor/pigmented epithelium interface, so the eye was hyperopic (far-sighted). The scale bar applies to b, c, and d.

The structural basis for the change in the focal length of the lens was investigated by examining sections through the lenses of fish of various ages, as illustrated in Fig. 8. The lens enlarged from 24 to 72 hpf, and the organization of the center changed progressively toward the concentric "onionskin" organization (see Fig. 6d) that characterizes the adult. At 24 hpf, the lens was solid, approximately spherical, and still attached to the skin. At 30 hpf, it was slightly larger, and the central core was clearly different histologically from the cuboidal epithelium on the outside. By 36 hpf, the concentric organization of the central cells was a little more pronounced, and the cuboidal epithelium was restricted to the side facing the cornea. The lenses at 48, 60, and 72 hpf were qualitatively similar; the center stained more intensely than the periphery, the central cytoplasmic layers were more numerous and thinner, and the side facing the retina was layered concentrically with the core. The lens acquired an egg shape, but this asphericity was absent in fresh lenses and therefore probably an artifact of histological preparation. The core stained progressively more densely, probably because of increased concentrations of crystallin proteins, the higher concentration of which produced a higher index of refraction and a shorter focal length (Pumphrey, 1961). When the core of a fresh lens was isolated from the less dense onionskin surrounding layers, the core formed an image (not shown), confirming that it was highly refractile, as Fernald and Wright (1983) have shown in the adult lens.

To relate the size of the retinal images of the gratings to the size of the images of the stripes on the drum, it is necessary to know the retinal magnification factor, defined as the number of micrometers on the retina that corresponds to a degree of visual angle. This cannot be reliably estimated from processed material (such as the sections of Fig. 8), so we analyzed optical sections through the center of the lens of living eyes oriented with the pupil parallel to the incident beam (Fig. 9). At 72 hpf, the lens and retina were adjacent to one another, separated only by the blood vessels on the retinal surface, and no vitreal space was apparent. The outer segments lay at the photoreceptor/pigmented epithelium interface (Figs. 10a and 10c), which was approximately 130 μm from the center of the lens. The circumference of a circle with that radius is 823 μm , so the retinal magnification factor for this eye was $(823 \mu\text{m}/360^\circ) = 2.28 \mu\text{m}/^\circ$ at the level of the outer segments. The stripes in Fig. 6c measured roughly 11 μm in width, which corresponds to $11/2.28 = 4.8^\circ$, much less than the smaller of the two stripe widths (22.5°) on the drum used in the tracking experiments. These comparisons confirm that the drum stripes must have been imaged clearly at 72 hpf and later.

Functional Retinal Anatomy

We compared 72 and 96 hpf retinas to see if any structural changes might account for the improvement in OKR over that period. We considered two possibilities. The first is an

enlargement of the functional retina, the part that actually senses the light. Detection of stripe movement requires that the functional retina be big enough to include both where a stripe first appears and where it appears later, so if the functional retina were very small, it might fail to detect movement. The second possibility is that the photoreceptor mosaic in the young retina was too coarse to resolve the stripes.

Extent of the functional retina. We determined the "retinal field" (the extent of the outside world that is imaged on the retina) by measuring the angle subtended by the entire retina relative to the lens center (Fig. 9). This was done in optical sections of living eyes of 72 and 96 hpf fish. The eyes of the two ages were similar, apart from the presence of a slight vitreal space, about 10 μm deep, that was present at 96 hpf but not at 72 hpf. The retinal field at 72 hpf was $218.3 \pm 2.6^\circ$, slightly larger than at 96 hpf ($212.1 \pm 3.1^\circ$, means and standard deviations of nasotemporal sections, $n = 5$ for both ages). This is the wrong direction to account for the improvement in OKR.

Only the central part of the anatomically defined "neural retina" serves a visual function. The peripheral part contains the proliferative zone (Muller, 1952; Johns, 1977), the ciliary margin, and the iris, none of which serve a photoreceptive function. The extent of the central functional region was assessed in histological sections of retinas from 72 and 96 hpf fish (Figs. 10c and 10d). The functional retina was assumed to correspond to that sector that contained outer segments (necessary to transduce the light) and the two plexiform layers (necessary to transmit the visual signal transsynaptically). At 72 hpf, the angular subtense of the functional retina was 139° and increased to 163° at 96 hpf. Both values should be adequate to detect stripes moving across the retina at a few degrees per second, so we can exclude the size of the functional retina as a determinative factor.

The assumption that cones with outer segments define the functional retina may be wrong; perhaps cone function was restricted to those cells with long outer segments. Cone outer segments first appear at 60 hpf (Branchek and Bre-Miller, 1984), but in a fairly restricted area of ventral retina. Our sections of 72 hpf retinas show that outer segments were present throughout the sector that included the plexiform layers, but they were shorter than those in the 96 hpf retinas (Figs. 10g and 10h). It is conceivable, but we think unlikely, that this elongation caused some of the improved performance; a definitive answer will await a developmental study of the physiology of these cones.

Photoreceptor mosaic. The resolving power of the visual system depends in part on the spacing of the cones—the closer the spacing, the finer the resolution. Sections parallel to the long axis of the cones (Figs. 10e and 10f) showed that they lay in a single layer with roughly constant density at all retinal eccentricities. Therefore, individual tangential sections through this layer will reveal the cone mosaic. Such sections were obtained through nasal retinas

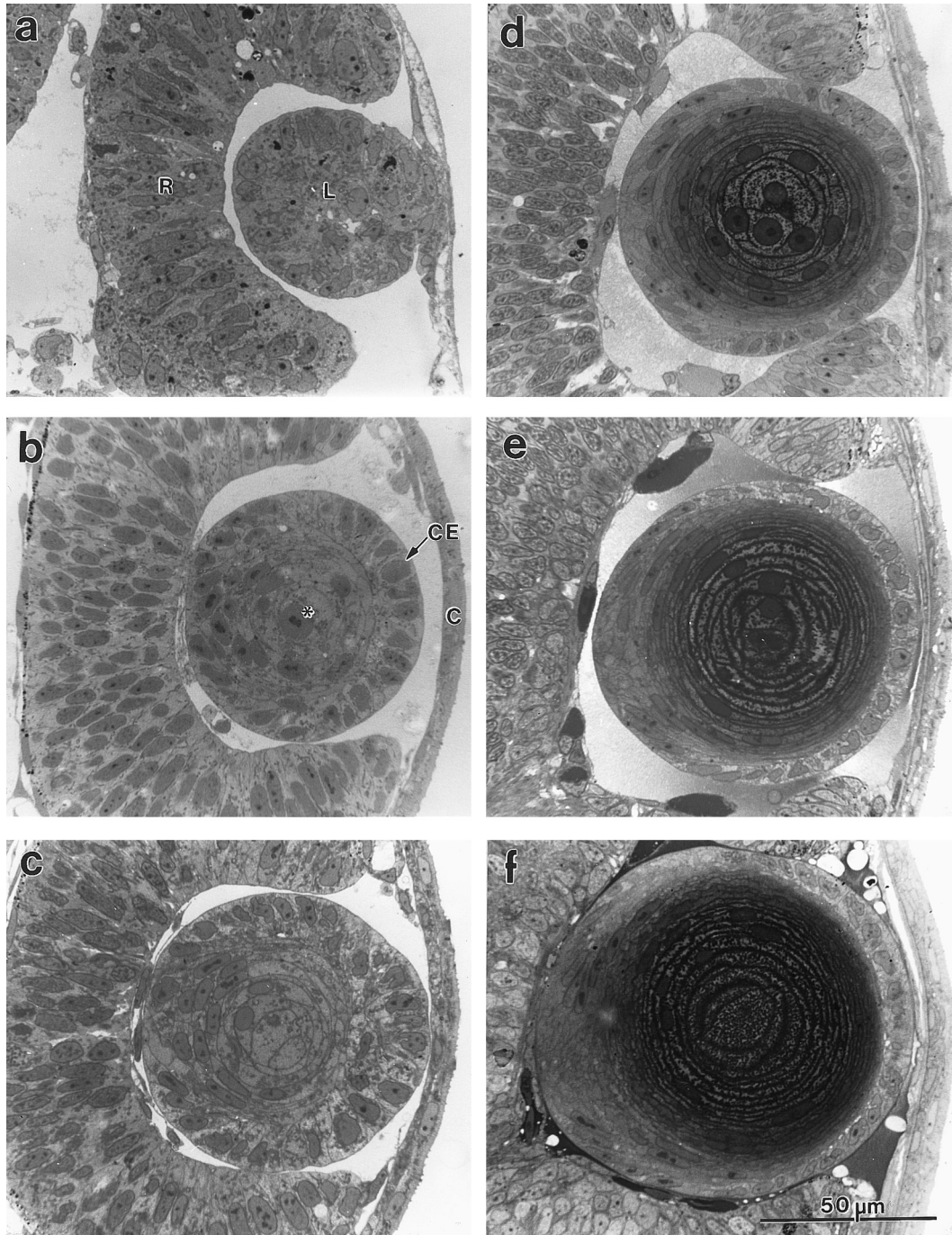


FIG. 8. Development of the lens. All panels show a dorsoventral section through the lens, dorsal up, lateral to the right. (a) 24 hpf. The lens (L) is spherical but still attached to the skin and surrounded on three sides by the retina (R). (b) 30 hpf. The cornea (C) is now separate, and the cuboidal epithelium (CE) on the lateral surface is distinct from the less structured core (*). (c) 36 hpf. The onionskin organization of the core is now apparent. (d) 48 hpf. The core is noticeably denser than the outside of the lens, and the cuboidal lateral epithelium contrasts with the concentrically organized medial side. (e) 60 hpf. The dense core has enlarged and the concentric laminae are thinner. The medial side begins to bulge, giving the lens an egg shape. (f) 72 hpf. Most of the surface of the lens now touches the retina, the egg shape remains, and the dense core is larger and denser. The scale bar in f applies to all panels.

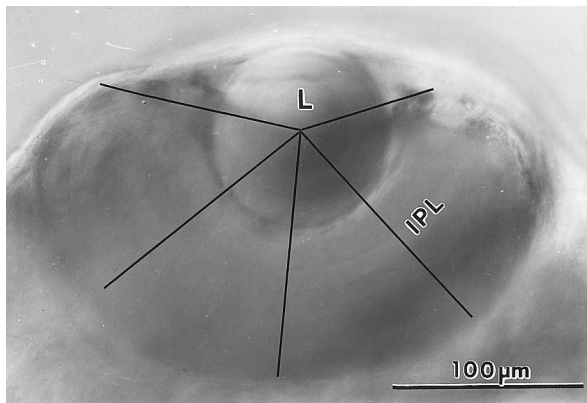


FIG. 9. Ocular morphology and retinal magnification factor. An optical horizontal section of the eye of a live 72 hpf zebrafish, anterior to the left, medial down. The differential interference contrast reveals the retinal inner plexiform layer (IPL). The lens (L) and the inner surface of the retina are in contact. The lines all originate at the center of the lens, the optical center of this eye. The upper two are connected to the peripheral edges of the retina, and the angle subtended by the retina is the retinal field. The lower lines are 125 μm long (lens radius \times 2.5), the predicted focal length of the lens, and extend to the vicinity of the photoreceptor/pigmented epithelium interface.

of 72 and 96 hpf fish (Figs. 10g and 10h), and the planimetric density (the number of cones per unit area, as viewed from the retinal surface) was measured by counting the nuclei and dividing by the area. It was slightly higher at 96 hpf (0.117 cones/degree²) than at 72 hpf (0.102 cones/degree²). The expression

$$\sqrt{(1/\text{planimetric density})}$$

gives the intercone separation, the average distance between the centers of neighboring cones in a square array. The values were 3.1° at 72 hpf and 2.9° at 96 hpf. Visual resolution is classically related to intercone separation by the "Helmholtz hypothesis," which states that two bright objects can be resolved by the cone mosaic only if their images illuminate separate cones that are separated by at least one unilluminated one. By this criterion, the 72 and 96 hpf cone mosaics could resolve gratings with stripes 3.1 and 2.9° wide, respectively, which is close to the behaviorally determined thresholds of 3–4.5° in 4 dpf zebrafish (Clark, 1981) and considerably smaller than the 22.5° stripes used above. Therefore, the slight reduction in the intercone distance between 72 and 96 hpf will not account for the big improvement in visual performance measured with 22.5 and 45° stripes.

The improvement in OKR between 72 and 96 hpf did not seem attributable to improved vision. OKR is a sensorimotor behavior, so the possibility remained that the improve-

ment was attributable to factors on the motor, rather than the sensory side, and that issue is addressed next.

Extraocular Muscles

The adult pattern of extraocular muscles is evident at 96 hpf and is shown in Fig. 11a. The superior and inferior oblique muscles originated together in the rostral orbit and inserted on the dorsal and ventral surfaces of the eye, respectively. The superior and inferior rectus muscles originated together in the caudal orbit and inserted immediately caudal to the insertions of the two obliques. The medial (anterior) rectus originated with the superior and inferior recti and extended between those two around the medial surface of the eye to insert on its anterior surface (Fig. 11b). The lateral (posterior) rectus originated farther caudally than the others, outside the orbit, and inserted on the posterior surface of the eye. All of the muscles except the medial rectus inserted at about the same equatorial plane (i.e., on a circle parallel to the plane of the pupil), but the medial rectus inserted more medially and so was not evident in most equatorial sections of the eye (Fig. 11c).

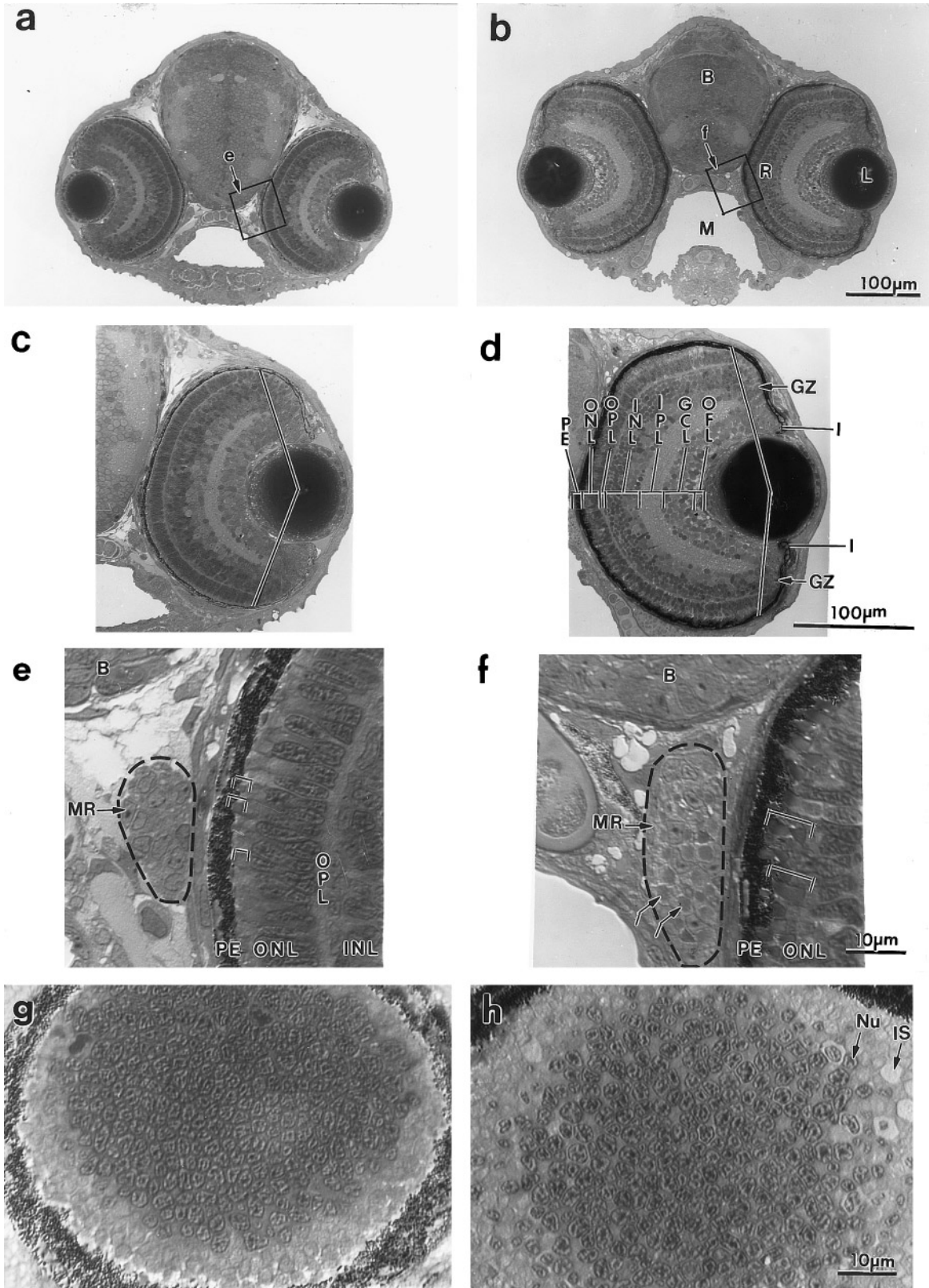
We examined fish of 48, 60, 66, 72, and 96 hpf to learn the state of development of the extraocular muscles. The 48 hpf fish showed no ZM-1 immunoreactivity. In the 60 hpf fish, the presumptive inferior oblique and medial rectus muscles were labeled, but both were incomplete, as they did not extend all the way to their origins. In the 66 hpf fish, the primordium of the lateral rectus muscle was also evident but also incomplete, again lacking the segment connecting to its origin. In both the 72 and 96 hpf fish, all six muscles were evident and extended their full lengths, but at 72 hpf they were generally thinner and stained less darkly than at 96 hpf. In transverse semithin sections (Figs. 10e and 10f) individual cells could be resolved, and they numbered about 20 at both ages, but the myofibrils were more numerous at the older age. This was confirmed electron microscopically; at 72 hpf, the extraocular muscles contained islands of thick and thin filaments, and by 96 hpf, they were more abundant and filled the sarcoplasm more completely (Figs. 11d and 11e).

We note that the onset of OKR occurred roughly simultaneously with the appearance of complete extraocular muscles (between 66 and 72 hpf) and suggest that the onset of OKR was limited by both this event and image formation. The muscular maturation between 72 and 96 hpf probably accounted for the improvement in OKR, as the larger muscles were undoubtedly stronger. They were also probably more resistant to fatigue than the smaller ones, and this may partly account for the fact that the older eyes spent more time tracking.

DISCUSSION

Integration of the Pieces: Which Step Comes Last?

Visual behavior depends on an intact neural circuit originating at the photoreceptors, passing through the brain, and



ending in the muscles causing the behavior, so the absence of a particular behavior could reflect a lack of function at any level of the circuit. What links were the last to be completed to enable the fish to make the two behaviors?

The answer is clearest for OKR, as it begins at about the same time that the eye becomes emmetropic and the extraocular muscles mature, and so we have concluded that these two were determinative. A third possibility is the arrival and maturation of retinal axonal arborizations at the appropriate location in the brain. Nine of the 10 retinorecipient sites receive retinal arbors by 66 hpf and the 10th by 72 hpf. It is possible that this last site [arborization field No. 8 (Burrill and Easter, 1994), which probably becomes either the *nucleus anterioris thalami* or the *nucleus pretectalis centralis*] specifically mediates horizontal OKR, but we know of no evidence for or against this possibility. If it did, it would therefore be a third limiting event.

The events limiting visual startle are less clear. The motor part of the reflex has been in place for more than a day before the visual stimulus can trigger it. The retina has outer segments and synapses, and the retinal axons have arborized in the tectum many hours before the onset of visual startle. Therefore, both the sensory and motor sides are probably functional in advance, and, if so, then the limiting step must be the formation of the sensory to motor link, a set of connections in the brain.

Image Formation

The larval eye is quite different structurally from that of the adult, which raises the possibility that image formation might be different in the two. First, the absolute size of the larval eye is smaller, roughly 0.2 mm in diameter vs several millimeters in the adult. Second, the relative sizes of the ocular contents are different from the adult. The lens and the retina have approximately the same thickness, ca. 100 μm , in contrast to the adult, in which the lens is typically more than 10 times as thick as the retina. The vitreal space is absent in the larva, as the inner limiting membrane is contiguous with the outer surface of the lens, while in the adult they are separated by a vitreal space that is many

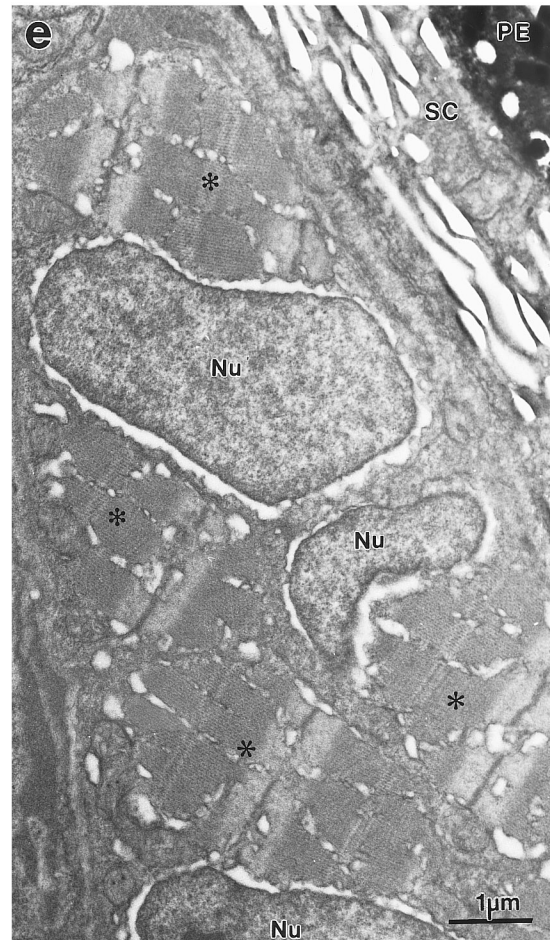
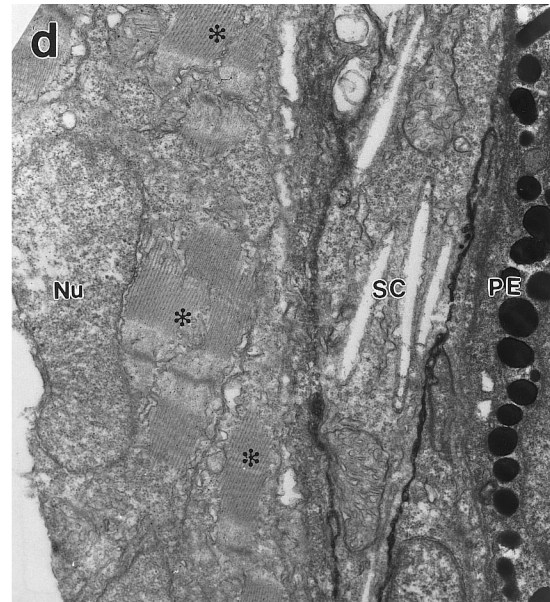
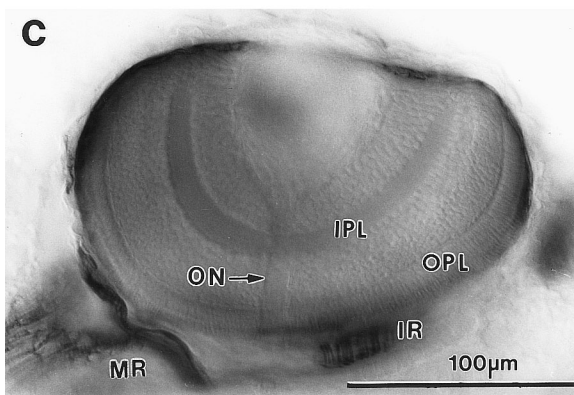
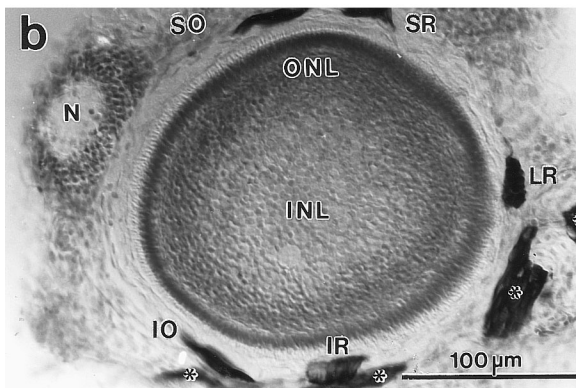
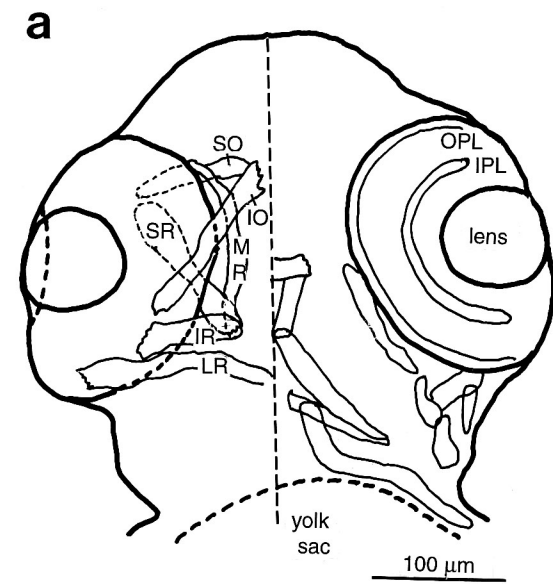
times thicker than the retina. The effects of these differences are analyzed below.

Small size. This is suspected to present a problem because diffraction of light degrades image quality, and degradation is increased in smaller apertures, which explains why small animals tend to have compound eyes (Barlow, 1964). In fact, the larval zebrafish eye is too large to be significantly affected by diffraction; the diameter of the entry pupil is about 100 μm , compared to 22 μm in honeybee (Barlow, 1964). The angular separation that two points must have if their images are to be resolved as separate is given by the equation

$$\theta = (1.22 \times \lambda)/d,$$

where θ is the minimum resolvable angle, the "Rayleigh limit," λ is the wavelength of light, and d is the diameter of the entry pupil. Assuming $\lambda = 600 \text{ nm}$ and $d = 100 \mu\text{m}$, then the Rayleigh limit for this eye is 25 min arc, about 0.5° . It will be recalled that the Helmholtz hypothesis predicts that the larval cone mosaics could not resolve stripes separated by less than twice the intercone spacing, or about 6° , which is 12-fold larger than 0.5° . Therefore, the larval eye casts a much finer image than its cone mosaic could resolve, and the cone mosaic is said to "undersample" the retinal image by $1/12 = 0.08$. Snyder *et al.* (1986) have analyzed this issue theoretically, taking into consideration photon noise and real-world quantum catches by the cones. They conclude that undersampling improves visual resolution, and they provide data from various terrestrial adult animals consistent with undersampling of about 0.4–0.5. The benefit of undersampling can be appreciated intuitively by considering the "Airy disk," the retinal image of a tiny point in the outside world. If the Rayleigh criterion matches the cone mosaic (sampling = 1.0), the Airy disk extends over about 10 cones, which seems undesirably blurry, but if the retina undersamples by 0.3, the image is almost fully restricted to a single cone, which seems preferable. Fernald and Wright (1985) have shown that the adult cichlid eye undersamples by about 0.1, very close to what we have found in the larval eye, so fish eyes are apparently quantita-

FIG. 10. Retinal development between 72 and 96 hpf. The left column shows sections from 72 hpf fish, the right from 96 hpf fish. Each horizontal pair of photos (a and b, c and d, etc.) have the same magnification, given by the scale bar on the right. (a, b) Transverse sections through the heads passing through the centers of the eyes. Dorsal is up. The brain (B), mouth (M), retina (R), and lens (L) are indicated. The boxes labeled e and f indicate the regions shown in e and f. (c, d) More highly magnified views of the eyes in the preceding micrographs. The various layers are indicated: pigmented epithelium (PE), outer nuclear layer (ONL), outer plexiform layer (OPL), inner nuclear layer (INL), inner plexiform layer (IPL), ganglion cell layer (GCL), and optic fiber layer (OFL). The older eye is larger and slightly more developed. The dark lines indicate the boundaries of the functional retina, the sector containing both plexiform layers and photoreceptor outer segments. Lateral to the functional retina lie the lens, the iris (I), and the retinal germinal zone (GZ). (e, f) More highly magnified views (see boxes in a and b) showing the outer segments (brackets) and the medial rectus muscle (MR) enveloped by dashed lines. In the older fish, the outer segments are longer and the medial rectus is larger and has more myofibrils (e.g., curved arrows). (g, h) Tangential sections through the outer nuclear layer of the nasal retina, showing the transversely cut cone nuclei (Nu) in the central field of both panels and the inner segments (IS) in the surrounding area.



tively different from the terrestrial adults that Snyder *et al.* (1986) considered. Although undersampling carries the risk of "aliasing," in which different images are perceived as similar (Wandell, 1995), the practical effect is not great in the aquatic world, where contrasts and spatial frequencies are low (D. R. Williams, personal communication).

Different relative sizes of lens, retina, and vitreal chamber. In the adult eye, the retina takes up so small a part of the projection distance that its role in image formation can usually be ignored, but when it occupies nearly all the space not occupied by the lens, one wonders if it might impede image formation. It does not. All adult fish lenses have a focal length equal to roughly $2.5\times$ the lens radius (Pumphrey, 1961; Walls, 1963). Consider the eye in Fig. 9a. Its lens has a radius of $50\text{ }\mu\text{m}$, and if it followed the same rule as adult lenses, its focal length would be $125\text{ }\mu\text{m}$. An image of an object at infinity would be formed at a plane $125\text{ }\mu\text{m}$ from the center of the lens, and as the illustration shows, that plane lies near the outermost edge of the retina, close to the outer segments, where we have shown that this lens does form an image. Thus, the larval and adult eyes are optically conformal, despite the big differences in both the absolute sizes of the eyes and the relative sizes of the retina, vitreous, and lens.

Comparable stages of lens and image development have not been studied in any other animals, to our knowledge, but the emmetropization has been examined at later stages in the eyes of birds and mammals. In those animals, the change from hyperopic to emmetropic is effected largely by altering the dimensions of the eye, e.g., the chick eye made hyperopic by a spectacle lens grows more than it normally would, thereby producing a distance from lens to retina that matches the focal length of the dioptric apparatus, and the hyperopic eye becomes emmetropic (Wallman *et al.*, 1987). Moreover, visual experience is essential to this correction (reviewed by Wallman, 1993). The early development in zebrafish is different on both counts: the adjustment from hyperopic to emmetropic was made by shortening the focal length of the lens (Figs. 6 and 7), and this shortening was independent of visual experience. The focal length is set by the radius and the internal refractive index profile of the lens (Pumphrey, 1961; Axelrod *et al.*,

1987). The lens radius changed very little, so the salient change must have been in the internal profile of the refractive index. This absence of an adaptive response by the lens is consistent with the most probable explanation of why the abnormally large eyes of the Black Moor goldfish are also extremely myopic (Easter and Hitchcock, 1986; Raymond *et al.*, 1988). They apparently suffer from excessive growth of the vitreal chamber without the compensatory growth of the lens that normally accompanies ocular growth throughout life (Easter *et al.*, 1977).

Our conclusion that the eye shifts from hyperopic to emmetropic contradicts an earlier study on the development of vision in fish larvae. Pankhurst *et al.* (1993) measured lens diameters in larvae of various ages, noted that the younger lenses were smaller, and inferred that the smaller lenses had correspondingly shorter focal lengths which would make the eyes myopic. They made no optical measurements in living eyes. We agree that the younger lenses have smaller diameters (see Fig. 8), but our studies of image formation showed that diameter was a poor predictor of focal length at this stage, so we do not accept their conclusion.

The abrupt shift of refractive state over the last few hours of the third day postfertilization has a counterpart in amphibian metamorphosis. When a tadpole shifts from life in water to the terrestrial habitat of the adult, the eye must shift from being functional in water, where the cornea is neutralized, to being functional in air, where the cornea bends the light. This shift occurs over the course of only a day or so and involves changes in the position, shape, and strength of the lens, without any change in the shape or size of the eye (Mathis *et al.*, 1988).

Finally, we note that the morphogenesis of the fish lens (Fig. 8), which we believe has not previously been described, differs from that of mammals and birds (reviewed by Piatigorsky, 1981). First, the lens forms by a delamination of cells from the ectoderm, rather than an invagination of the lens placode, and so the presumptive lens is solid from its first appearance, never passing through a stage as a hollow lens vesicle. Second, the primary lens fibers in the fish lens, the ones at the center, are oriented randomly or wrapped around the core, but never take the linear shape typical of

FIG. 11. Extraocular muscles. (a) *Camera lucida* drawing of ventral view of the head of 96 hpf fish which had been reacted against the ZM-1 antibody. To the right of the midline (dashed line), the eye with its lens and two plexiform layers is indicated, as are the head muscles not associated with the eye. To the left, the six extraocular muscles are shown, with the convention that more ventral structures are outlined in solid, and masked outlines (of eye or muscles) are dashed. The six muscles are the superior oblique (SO), the inferior oblique (IO), the medial rectus (MR), the superior rectus (SR), the inferior rectus (IR), and the lateral rectus (LR). (b) Parasagittal (equatorial) section of a 96 hpf eye, dorsal up, rostral left, with approximately transverse sections of five of the six extraocular muscles. Only the medial rectus is missing, because it inserts more medially than the others. The nose (N) is indicated, as are the muscles not associated with the eye (*). (c) Optical section in the horizontal plane of a whole-mounted 96 hpf fish, lateral up, rostral left, showing the belly of the inferior rectus and the insertion of the medial rectus. The plexiform layers and the intraretinal optic nerve (ON) are also shown. (d, e) Electron micrographs of oblique sections through extraocular muscles in 72 and 96 hpf fish, respectively. The scale bar in e applies to both. The melanin in the pigmented epithelium (PE) and the reflective plates in the sclera (SC) provide landmarks for the edge of the eye. The nuclei (Nu) and myofibrils (*) are indicated. The older muscle is larger and more fully packed with myofibrils than the younger.

the primary lens fibers in birds and mammals, perpendicular to the cornea.

Polarization of OKR

The observation that OKR was always in the appropriate direction, even in the visually deprived fish, has important implications for the early wiring of the nervous system and leads to interesting predictions about fish with genetically altered brains. Briefly, if the eyes are to move in the same direction as the drum, the retinas must produce signals that correctly code the direction of the drum movement. A lot of studies on both amphibians and fish have shown that when the polarity of the signal is altered surgically, e.g., by causing one eye to project to the wrong side of the brain, the eyes move as in OKR and the animal circles continuously, locked in a maladaptive positive feedback loop. Such unstable behavior is the direct consequence of an altered polarity caused by sending the signal to the wrong side of the brain (Sperry, 1945; Easter and Schmidt, 1977). All previous experiments of this sort have been carried out on visually experienced animals and illustrate the immutability of the polarity that had been established prior to the surgery. However, these experiments do not tell how the polarity was initially set, i.e., on the basis of visual experience or not. Our observations are novel in that they document the polarity at the earliest possible time, and while they suggest that it is established prior to experience, they do not test that hypothesis directly. Genetically altered zebrafish with retinal axons projecting ipsilaterally rather than contralaterally would provide an excellent test, because in their brains the miswiring has occurred in advance of visual experience. Such fish have been produced (F. Bonhoeffer, personal communication) and should be instructive with respect to this question. If the polarity is set independently of visual experience, then these miswired fish should have incorrect polarity and show horizontal circus movements and a spontaneous resting ocular nystagmus. If the polarity is set initially on the basis of a functional validation of visual experience, then these fish should show normal visuomotor behavior, including OKR.

SUMMARY

We have shown that vision develops rapidly over the course of 2 days, from the time that the first retinal cells withdraw from the mitotic cycle to the time that the eyes begin to be able to follow a moving target. Simple light/dark distinctions across time become possible toward the end of the third day of life, and form-vision begins a few hours later. Visual function is made possible by the nearly simultaneous acquisition of a good retinal image, functional extraocular muscles, and projections from the retina to all the retinorecipient targets in the brain. This all happens around the morning of the first posthatching day, and this

is when the visual life of the zebrafish can properly be said to begin.

ACKNOWLEDGMENTS

We thank Professor Monte Westerfield of the University of Oregon for the gift of the monoclonal antibody ZM-1, Ms. Celeste Malinoski for extensive technical support and instruction, Dr. Dan Green for help with the measurements of luminance, and Drs. Grant Mastick and Charlotte Mistretta for comments on the manuscript. G.N.N. was supported in part by a training grant from NSF (DIR-9014275). This research was supported by a research grant from the National Eye Institute (EY-00168) to S.S.E., Jr.

REFERENCES

- Axelrod, D., Lerner, D., and Sands, P. J. (1988). Refractive index within the lens of a goldfish eye determined from the paths of thin laser beams. *Vision Res.* **28**, 57–65.
- Barlow, H. B. (1964). The physical limits of visual discrimination. *Photophysiology* **2**, 163–202.
- Bodick, N., and Levinthal, C. (1980). Growing optic nerve fibers follow neighbors during embryogenesis. *Proc. Natl. Acad. Sci. USA* **77**, 4374–4378.
- Branchek, T. (1984). The development of photoreceptors in the zebrafish, *Brachydanio rerio*. II. Function. *J. Comp. Neurol.* **224**, 116–122.
- Branchek, T., and BreMiller, R. (1984). The development of photoreceptors in the zebrafish, *Brachydanio rerio*. I. Structure. *J. Comp. Neurol.* **224**, 107–115.
- Burrill, J. D., and Easter, S. S., Jr. (1994). The development of the retinofugal projections in the embryonic and larval zebrafish (*Brachydanio rerio*). *J. Comp. Neurol.* **346**, 583–600.
- Burrill, J. D., and Easter, S. S., Jr. (1995). The first retinal axons and their microenvironment in zebrafish: Cryptic pioneers and the pre-tract. *J. Neurosci.* **15**, 2935–2947.
- Charman, W. N., and Tucker, J. (1973). The optical system of the goldfish eye. *Vision Res.* **13**, 1–8.
- Clark, D. T. (1981). Visual responses in developing zebrafish. Ph.D. Thesis, University of Oregon, Eugene.
- Easter, S. S., Jr. (1971). Spontaneous eye movements in restrained goldfish. *Vision Res.* **11**, 333–342.
- Easter, S. S., Jr. (1972). Pursuit eye movements in goldfish (*Carassius auratus*). *Vision Res.* **12**, 673–688.
- Easter, S. S., Jr., and Hitchcock, P. F. (1986). The myopic eye of the Black Moor goldfish. *Vision Res.* **26**, 1831–1833.
- Easter, S. S., Jr., and Nicola, G. N. (1995). The development of vision and eye movements in zebrafish (*Danio rerio*). *Invest. Ophthalmol. Vis. Sci.* **36**(Suppl.), 762.
- Easter, S. S., Jr., and Schmidt, J. T. (1977). Reversed visuomotor behavior mediated by induced ipsilateral retinal projections in goldfish. *J. Neurophysiol.* **40**, 1245–1254.
- Easter, S. S., Jr., Johns, P. R., and Baumann, L. R. (1977). Growth of the adult goldfish eye—I: Optics. *Vision Res.* **17**, 469–477.
- Fernald, R. D., and Wright, S. E. (1983). Maintenance of optical quality during crystalline lens growth. *Nature* **301**, 618–620.
- Fernald, R. D., and Wright, S. E. (1985). Growth of the visual system

- in the African cichlid fish, *Haplochromis burtoni*. *Optics. Vision Res.* 25, 155–161.
- Grunwald, D. J., Kimmel, C. B., Westerfield, M., Walker, C., and Streisinger, G. (1988). A neural degeneration mutation that spares primary neurons in the zebrafish. *Dev. Biol.* 126, 115–128.
- Johns, P. R. (1977). Growth of the adult goldfish eye: III. Source of the new retinal cells. *J. Comp. Neurol.* 176, 343–358.
- Kimmel, C. B., Patterson, J., and Kimmel, R. O. (1974). The development and behavioral characteristics of the startle response in the zebra fish. *Dev. Psychobiol.* 7, 47–60.
- Larison, K. D., and BreMiller, R. (1990). Early onset of phenotype and cell patterning in the embryonic zebrafish retina. *Development* 109, 567–576.
- Mathis, U., Schaeffel, F., and Howland, H. C. (1988). Visual optics in toads (*Bufo americanus*). *J. Comp. Physiol. A* 163, 201–213.
- Müller, H. (1952). Bau und Wachstum der Netzhaut des Guppy (*Lebistes reticulatus*). *Zool. Jb.* 63, 275–324.
- Nawrocki, L. W. (1985). Development of the neural retina in the zebrafish, *Brachydanio rerio*. Ph.D. Thesis, University of Oregon, Eugene.
- Pankhurst, P. M., Pankhurst, N. W., and Montgomery, J. C. (1993). Comparison of behavioural and morphological measures of visual acuity during ontogeny in a teleost fish, *Forsterygion varium*, tripterygiidae (Forster, 1801). *Brain Behav. Evol.* 43, 178–188.
- Pumphrey, R. J. (1961). Concerning vision. In "The Cell and the Organism: Essays presented to Sir James Gray". (J. R. Ramsay and V. B. Wigglesworth, Eds.). Cambridge Univ. Press, London.
- Raymond, P. A., Barthel, L. K., and Curran, G. A. (1995). Developmental patterning of rod and cone photoreceptors in embryonic zebrafish. *J. Comp. Neurol.* 359, 537–550.
- Raymond, P. A., Hitchcock, P. F., and Palopoli, M. F. (1988). Neuronal cell proliferation and ocular enlargement in Black Moor goldfish. *J. Comp. Neurol.* 276, 231–238.
- Snyder, A. W., Bossomaier, T. R. J., and Hughes, A. (1986). Optical image quality and the cone mosaic. *Science* 231, 499–501.
- Sperry, R. W. (1943). Effect of 180 degree rotation of the retinal field on visuomotor coordination. *J. Exp. Zool.* 92, 263–279.
- Sperry, R. W. (1945). Restoration of vision after cross union of optic nerves and after contralateral transplantation of eye. *J. Neurophysiol.* 8, 15–28.
- Springer, A. D., Easter, S. S., Jr., and Agranoff, B. W. (1977). The role of the optic tectum in various visually mediated behaviors of goldfish. *Brain Res.* 128, 393–404.
- Wallman, J. (1993). Retinal control of eye growth and refraction. *Prog. Retinal Res.* 12, 133–153.
- Wallman, J., Gottlieb, M. D., Rajaram, V., and Fugate-Wentzek, L. A. (1987). Local retinal regions control local eye growth and myopia. *Science* 237, 73–77.
- Wandell, B. A. (1995). "Foundations of Vision," pp. 57–63. Sinauer Associates, Sunderland, MA.
- Westerfield, M. (1993). "The Zebrafish Book." Univ. Oregon Press, Eugene, OR.

Received for publication July 31, 1996

Accepted September 23, 1996